SECTION 10

N72-29311

A MULTISPECTRAL METHOD OF MEASURING SEA SURFACE TEMPERATURES FROM SATELLITES

by

William E. Shenk
and
Vincent V. Salomonson
Laboratory for Meteorology
and Earth Sciences
Goddard Space Flight Center
Greenbelt, Md. 20771

INTRODUCTION

High chlorophyll concentrations are associated with areas of the oceans where nutrients are plentiful. Nutrients are supplied from the ocean bottom in regions of upwelling characterized by relatively low temperatures. Algae growth is aided in coastal waters where relatively high temperatures are found. Therefore, measurements of sea surface temperatures are important in the detection of the areas of upwelling and warm coastal waters. As a result of satellite measurements it has been possible to study the temporal sea surface temperature fluctuations in areas where, before the satellite observations, changes were virtually unknown. A good example is the study of the strong upwelling off the Somali Coast. Upwelling along the northeast African coast begins in connection with the development of the southwest monsoon in May. From May to July the temperature gradient increases and the relatively cold temperatures, which first appear near the coast, move offshore to form an anticyclonic gyre that has a characteristic diameter of about 600 km. Figure 1 shows a view of the gyre on July 3, 1966 where the equivalent blackbody temperature pattern (uncorrected for atmospheric effects) was obtained from the 3.5-4.1 μm measurements of the Nimbus 2 High Resolution Infrared Radiometer (HRIR). The gyre is fully developed with a temperature gradient of 5°K and the width of the cold temperature tongue is about 100 km. The lower portion of Figure 1 depicts chlorophyll concentrations measured during a similar event by an Indian Ocean expedition vessel. Highest concentrations are seen in the meridional cross section near the coast and in the offshore area of the gyre whereas the minimum concentrations were found in the relatively warm waters in between.

There are two problems associated with remotely sensing the sea

surface temperature with infrared measurements that dominate the total error budget. There are the effects of the atmosphere on the emission in an atmospheric window and clouds. The greatest potential error is obscuration of the sea surface by clouds since the emission from the clouds can come from a wide temperature range that is associated with the cloud top levels. Thus, it is imperative that a remote sensing technique for ocean temperature measurement contain a means for determining that the emitted energy is coming from a cloud free source. A multispectral technique has been developed (Shenk and Salomonson, 1972) using the measurements from the Nimbus 2 Medium Resolution Infrared Radiometer (MRIR) that tests for the presence of clouds before accepting the concurrent window infrared emission from what was assumed to be sea surface and the intervening cloud free atmosphere.

METHOD

The Nimbus 2 MRIR was a scanning radiometer operating in 5 spectral regions. All observations in these five channels were geographically registered at the same point and had an instantaneous field-of-view at the subsatellite point of 55 km. Three of these spectral regions were used in this study; namely, the 0.2-4.0 μm region where the observed reflectivity of clouds is generally quite high relative to the ocean surface, the 6.4-6.9 μm region that responds to upper tropospheric water vapor and clouds thereby offering a descriminator for the presence of cirrus, and the 10-11 μm window region permitting the observation of sea surface temperature in cloud free areas. This approach consists of establishing thresholds for the 0.2-4.0 μm reflectance channel and the 6.4-6.9 μm water vapor channel which indicate when a particular concurrent observation in the 10-11 μm channel is cloud free. In this study several threshold combinations in the reflectance and water vapor channels were selected based on observed frequency distributions of the MRIR observations taken from four relatively cloud free days during a one-month period from mid-June to mid-July, 1966 over an area encompassed by the latitudes from 30-50°N and longitudes stretching from 30°W to a line that was parallel to and no closer than 50 nautical miles (more than 1 MRIR resolution element diameter) from the United States coastline. The four relatively cloud free days were selected over this region by looking at the pictures taken by the Advanced Vidicon Camera System (AVCS) on the Nimbus 2 satellite which had a nominal spatial resolution of 0.9 km.

Figure 2 shows the frequency distribution of the observations taken for the four days in the reflectance region. Normalization of the 0.2-4.0 μm reflected energy for solar zenith angle was accomplished with the expression:

$$\bar{r} = \frac{\pi \bar{N}}{H^* \cos \delta}$$

where $\bar{r}$ is the normalized reflectance, $\bar{N}$ is the effective radiance, H^* is the effective solar constant and δ is the solar zenith angle. The strong peak at low reflectances corresponds to the normalized reflectances occurring over the ocean surface. Larger reflectances are associated with clouds and cloud/clear sky combinations. The cloud-no cloud threshold was positioned at a point displaced a distance Δr on the high reflectance side of the frequency peak resulting from observations from what was most likely the cloud-free ocean surface. The magnitude of Δr was set equal to the difference between the lowest observed reflectance and the reflectance corresponding to the above-mentioned frequency peak. In Figure 1 there were no $\bar{r}$ values less than 3. Thus, with the frequency peak at $\bar{r} = 6$, $\Delta r = 3$ and the reflectance cutoff was placed at $\bar{r} = 9$. The Δr on the low reflectance side of the peak was assumed to be produced by random instrument noise and other minor factors such as sea surface glitter.

The layer emitting most of the radiation from which the sensed radiance emanated in the 6.4-6.9 μm spectral band is from 7-11 km for a U.S. Standard Atmosphere with 2.0 cm of precipitable water. This is within or slightly below the level where cirrus clouds are generally located. When this layer was relatively dry the radiation was emitted from a slightly lower layer and thus, in general, from a region of warmer temperatures. With a dry upper troposphere the likelihood of the presence of cirrus clouds was considered to be small.

A frequency distribution approach was also followed in setting the thresholds for the water vapor channel equivalent blackbody temperature observations. Two separate criteria were used to establish these thresholds. One criterion consisted of setting the threshold at the 1σ location on the warm side of the mean of the water vapor channel observations that were taken over specified latitude zones (Figure 3). The second criterion was less restrictive and the threshold was established at the 70% point of the cumulative frequency distribution of equivalent blackbody temperatures (where the cumulative frequency curve started at the lowest temperatures).

RESULTS AND DISCUSSION

Using the threshold selection techniques described above, Nimbus 2 window channel observations, which were objectively selected as being cloud free, were collected over the month period for the area in the

Atlantic already described. Using different threshold combinations and ranges in radiometer observation nadir angle (η), 4 different sets of these measurements were assembled and composited on 1:5 million Mercator grid print maps (Nimbus Project, 1966[2]) with a grid point spacing of 0.625° of longitude.

For comparison purposes with the window radiation measurements all available ship observations of sea surface temperature were obtained for the time period already specified and from 31-43°N and 58°W westward to the U.S. coast. These ship observations (about 4500) were composited on the same map projection and scale as that employed for the radiometric observations. The differences between the ship observed temperatures and the window channel temperatures at a grid point were computed wherever 4 or more radiometric and ship observations occurred. The results were tabulated in histograms for each of four equally-spaced latitude bands from 31-43°N. Figure 4 shows the results for the set with the most relaxed thresholds where the 70% cumulative frequency threshold for the water vapor channel was used and the nadir angle limits were 0-50°. The differences between the ship observations and the observed window equivalent blackbody temperatures (ΔT) are caused by atmospheric effects. These effects were greatest in the 31-34°N region where the frequency peak occurs at ΔT = 8K whereas ΔT = 4-5K for the frequency peak at 40°N-43°N. The dispersion in the results within a latitude band occur because of variability in atmospheric attenuation effects, η, some nonconcurrence in time of the ship and radiometric observations, possible clouds, and random errors in the ship reports. The best comparisons were achieved between 31-34°N where a total dispersion of 2.0K about the mean difference between the ship and radiometer equivalent blackbody temperatures (ΔT) occurred. Larger dispersions further north were believed to be mostly attributable to greater ocean temperature fluctuations occurring during the month period. Despite the relaxed water vapor channel threshold and the wide nadir angle limits the results were similar to those for the other sets with the more stringent thresholds.

Another important result was an experiment to examine the possibility of using just one of the two cloud filtering channels. The conclusion was that the two channel cloud filter was substantially superior to the use of either of the channels alone.

The magnitude of the atmospheric correction to the sensed window radiance depends on the spectral interval, the vertical temperature profile, particulate matter, η, and the vertical distribution of the absorbing constituents. For the Nimbus 2 MRIR window channel the principal absorbing constituents are ozone and water vapor. Therefore, the smaller differences between observed ship temperatures and the window equivalent blackbody temperatures at the higher latitudes was

probably caused by smaller atmospheric water vapor content and colder vertical temperature profiles. Any difference in the particulate concentration as a function of latitude was uncertain.

In order to correct the radiometric observations for the atmospheric effects, a stepwise multiple regression approach was employed. This permitted the evaluation of a simple linear correlation which fitted each grid print window channel radiometric observation average to each grid print ship observation average. In addition, the multiple correlation approach was used to assess the utility of including not only the two parameters just mentioned, but also the observations in the reflectance and water vapor channels, and the nadir angle at which the measurements were made. The multiple regression approach permitted the specification of the ship sea surface temperatures to an r.m.s. error of approximately 1.5K for all latitudes. When the results were stratified into two equal latitude bands, the temperatures in the lower latitudes could be determined to approximately 1K.

The two regression equations were then used to process the radiometric information and arrive at a map of sea surface temperature. This map is shown in Figure 5. The corrected sea surface temperature map shows the basic ocean features that would be expected in the June-July period over the western North Atlantic. A short distance east of the United States coast is the warm axis of the Gulf Stream with sea surface temperatures of about 300K. The strong thermal gradient of about 10K occurs in connection with the north wall of the Gulf Stream just north of 40°N. This gradient is not as steep as it normally is on a given day due to the one month data collection period and the spatial resolution of the MRIR.

Other investigations have successfully employed this technique over different oceanic regions. Figure 6 shows the temperature gradients for a consecutive 3-week period in June-July, 1966 over the southern Indian Ocean, from 10° to 45°S (Shenk and Szekielda[3]). The 10-11 um equivalent blackbody temperatures have not been corrected for atmospheric effects. The radiation measurements detected the Agulhas Current flowing southwestward along the African Coast to 38°S. An area of upwelling was located just off the south coast of Africa and north of the warm axis of the Agulhas Current.

The oceanic polar front is pronounced between 40-45°S which is associated with a convergence of the surface currents. Thus, the front separates the cold polar surface water from the warmer water masses of the lower latitudes. The center of this front lies in the Indian Ocean in the region where the water temperatures are, according to the uncorrected satellite data, in the range of 281-283°K. This cold water is found in the tropics at a depth of 300-400 m and in the

subtropics between 500-1000 m which originates at the surface at about 40°S.

The analysis of remotely sensed radiation data from the satellite gave a temperature gradient at 52°E and 43°S of 0.055C km^{-1}. This is a sharper horizontal gradient than that associated with the upwelling region along the Somali Coast and more pronounced than in the nautical charts for this area. Considering the ground resolution of the radiometer and the time period of approximately three weeks during which the radiation data were sampled, it is concluded that the temperature gradient should be still greater if synoptic measurements over shorter periods are made and that the polar front had a very stable position. This gradient is comparable with similar temperature gradients in the Gulf Stream. The Gulf Stream temperature boundary oscillates so much that a temperature analysis over a few weeks substantially smoothes the original sharp temperature gradients.

Szekielda[4] has discussed in more detail upwelling along the south African west and south coasts. Figure 7 shows his analysis from mid-May to mid-June, 1966. The prominent warm axis of the Agulhas Current is seen to extend south of 40°S with a small area of upwelling (285°K uncorrected isotherm) appears just off the south African Coast. A stronger region of upwelling produced by southerly winds is found associated with the Benguela Current along the west coast between 30°S and the Cape of Good Hope.

CONCLUSIONS

A multispectral technique has been developed which independently tests for the presence of clouds before a registered window radiance measurement is accepted as coming from the sea surface and the intervening atmosphere. The spatial resolution of ocean temperature mapping can be the same as that of the radiometer. With the 55 km subsatellite track resolution of the Nimbus 2 MRIR, current boundaries and upwelling areas have been successfully identified. Knowledge of the position of these regions and temperatures within them are important to the detection of areas of high chlorophyll concentrations.

These three registered channels will hopefully be flown on radiometers that are proposed for space flight on the TIROS N, ATS-G, and EOS missions. The spatial resolutions will vary from 0.9 km (TIROS-N) to 11 km (ATS-G) for the 11 μm channel. In the interim it may be possible to implement this technique where the appropriate channels are flown on the same satellite but are not part of the same instrument (Nimbus E).

REFERENCES

1. Shenk, W. E. and V. V. Salomonson, 1972: "A Multispectral Technique to Determine Sea Surface Temperature Using Nimbus 2 Data", J. of Phys. Ocean. (to be published in April, 1972).

2. Nimbus Project, 1966: "Nimbus 2 Users' Guide", Goddard Space Flight Center, Greenbelt, Maryland, 229p.

3. Shenk, W. E. and K-H. Szekielda, 1971: "Satellite Ocean Temperature Analysis of the Indian Ocean", Paper presented at the Symposium on Indian Ocean and Adjacent Seas, Cochin, India, Jan. 12 - 18, 1971.

4. Szekielda, K-H., 1971: "Upwelling Studies with Satellites", NASA X-651-71-298, 17p.

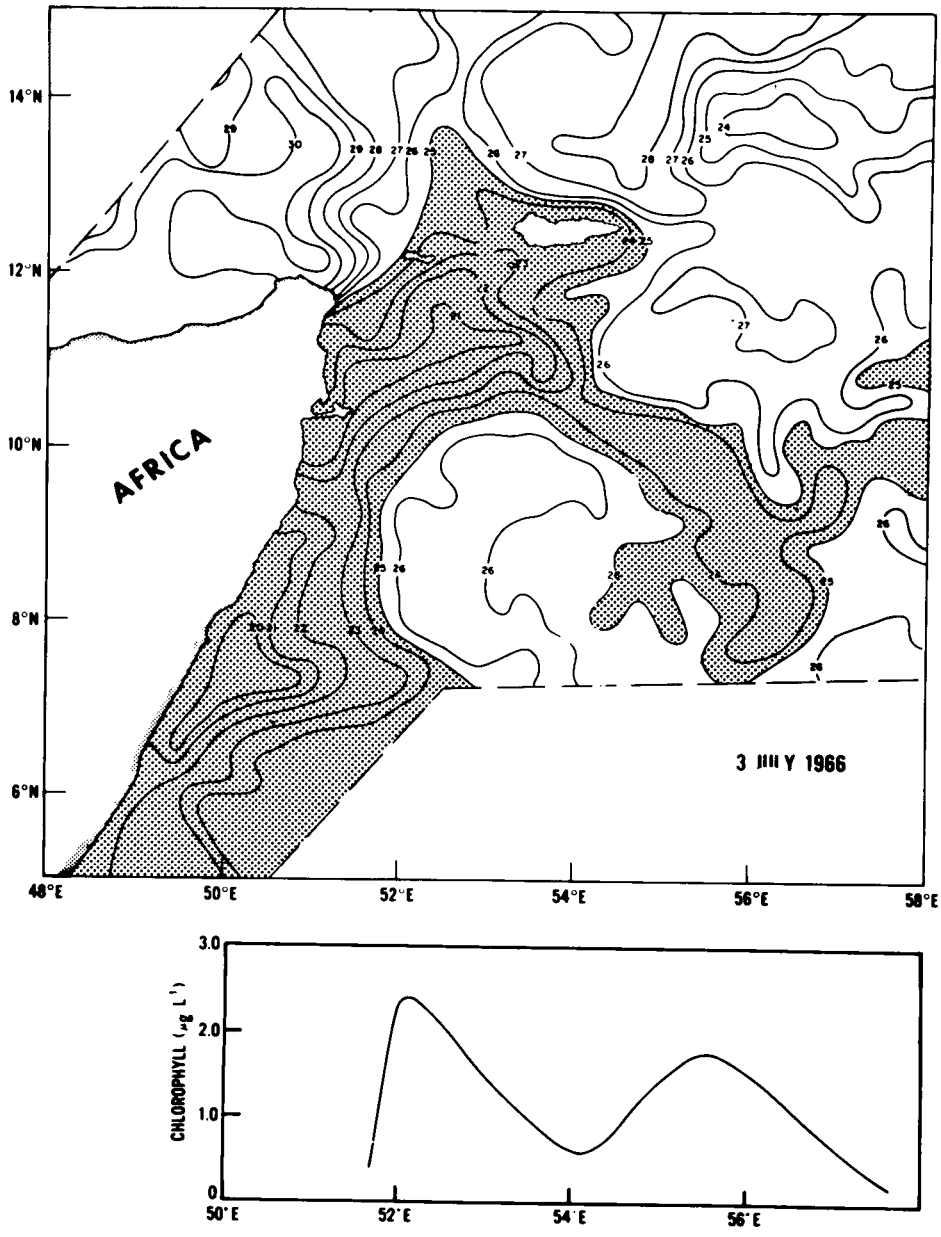

Figure 1 - Top - Nimbus 2 High Resolution Infrared Radiometer Equivalent Blackbody Temperatures (uncorrected for atmospheric effects) of the fully developed upwelling gyre off the Somali Coast on July 3, 1966 (after Szekielda). Isotherms are in °C and equivalent blackbody temperatures $\leq$25°C within the gyre are shaded.

Bottom - An east-west cross-section of chlorophyll concentrations recorded by an Indian Ocean Expedition vessel during a similar event.

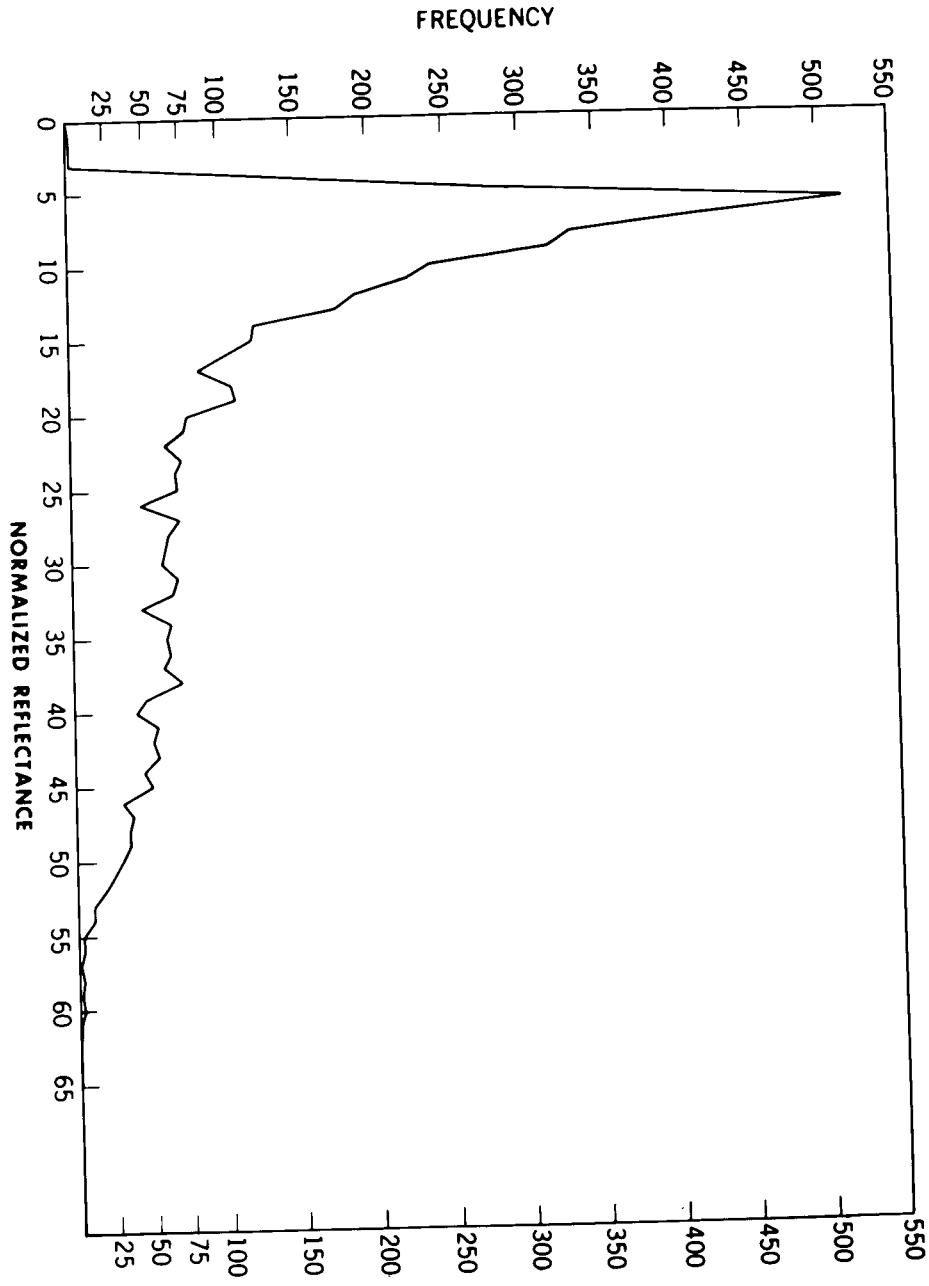

Figure 2 - Frequency distribution of normalized reflectance measurements from the 0.2-4.0 μm channel of the Nimbus 2 Medium Resolution Infrared Radiometer for 4 relatively clear days over the western North Atlantic between mid-June and mid-July, 1966.

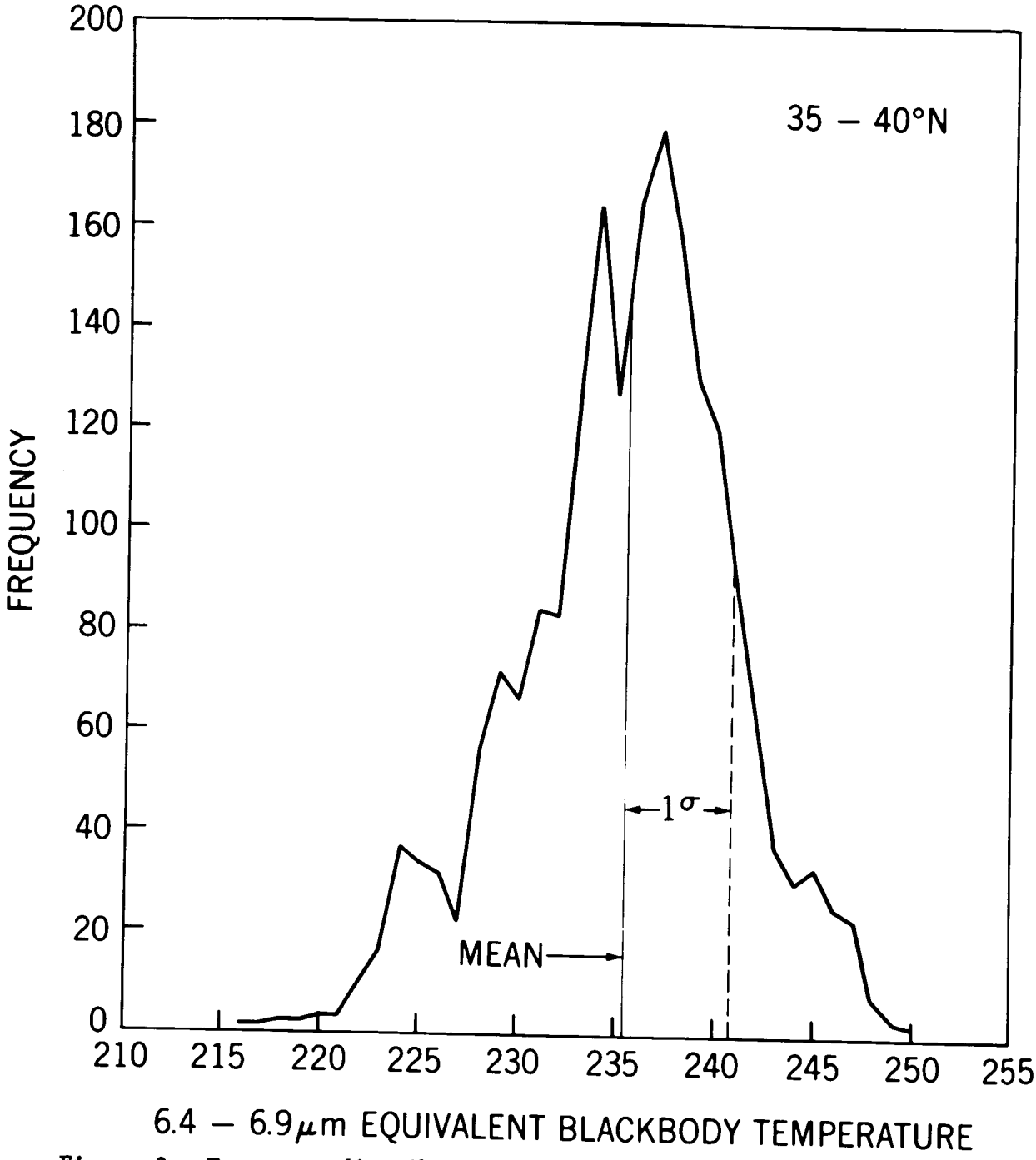

Figure 3 - Frequency distribution of 6.7 μm equivalent blackbody temperatures ($T_{BB's}$) for the same 4 days as in Figure 2. The mean and 1 σ to the warm side of the mean are indicated where the $T_{BB's}$ on the warm side of the 1 σ point were assumed to be associated with a cloud free upper troposphere.

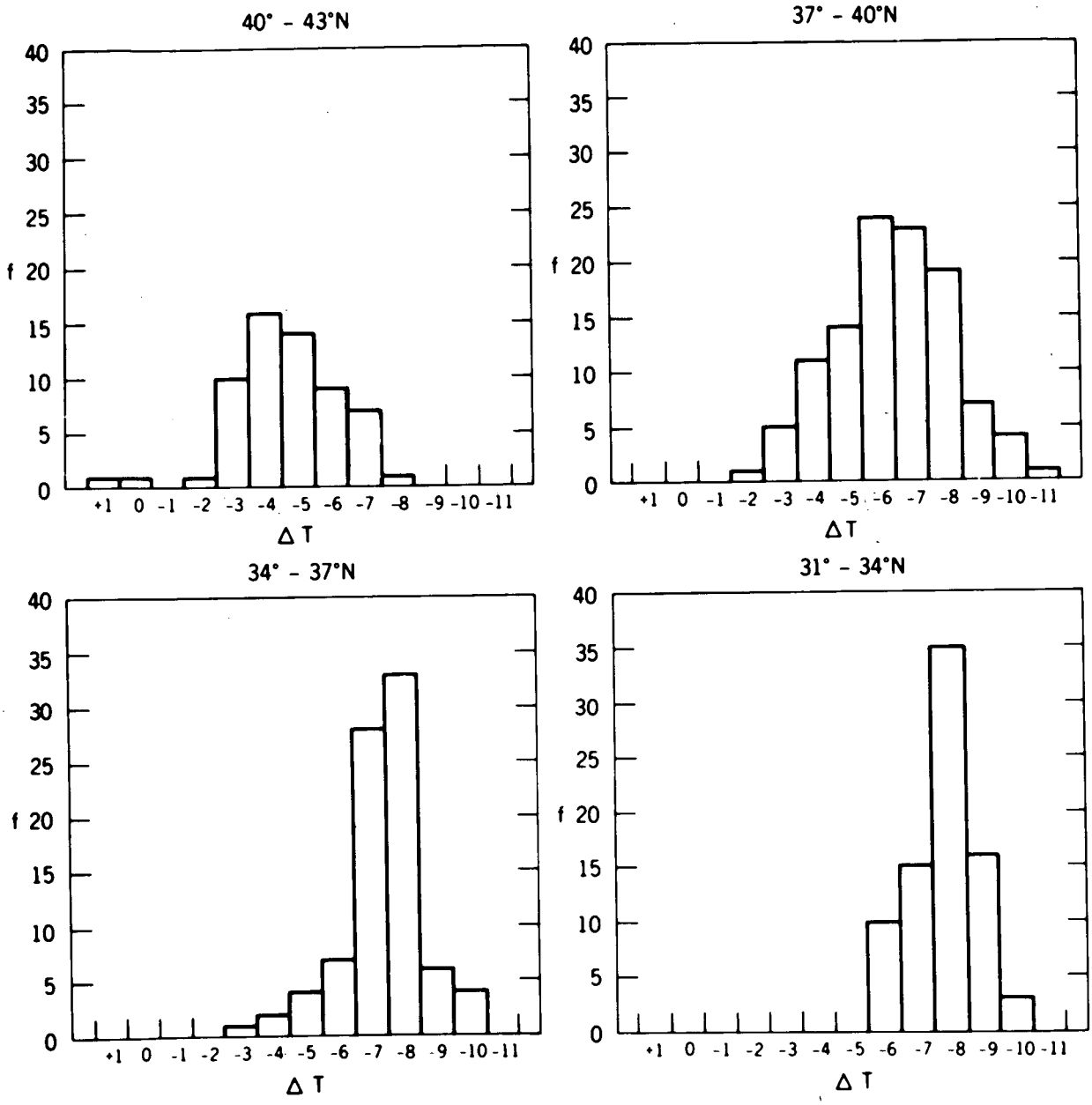

Figure 4 - Frequency distributions for 4 equally spaced latitude bands over the western North Atlantic of the difference between ship sea surface temperatures and 10-11 μm window equivalent blackbody temperatures associated with assumed cloud free conditions.

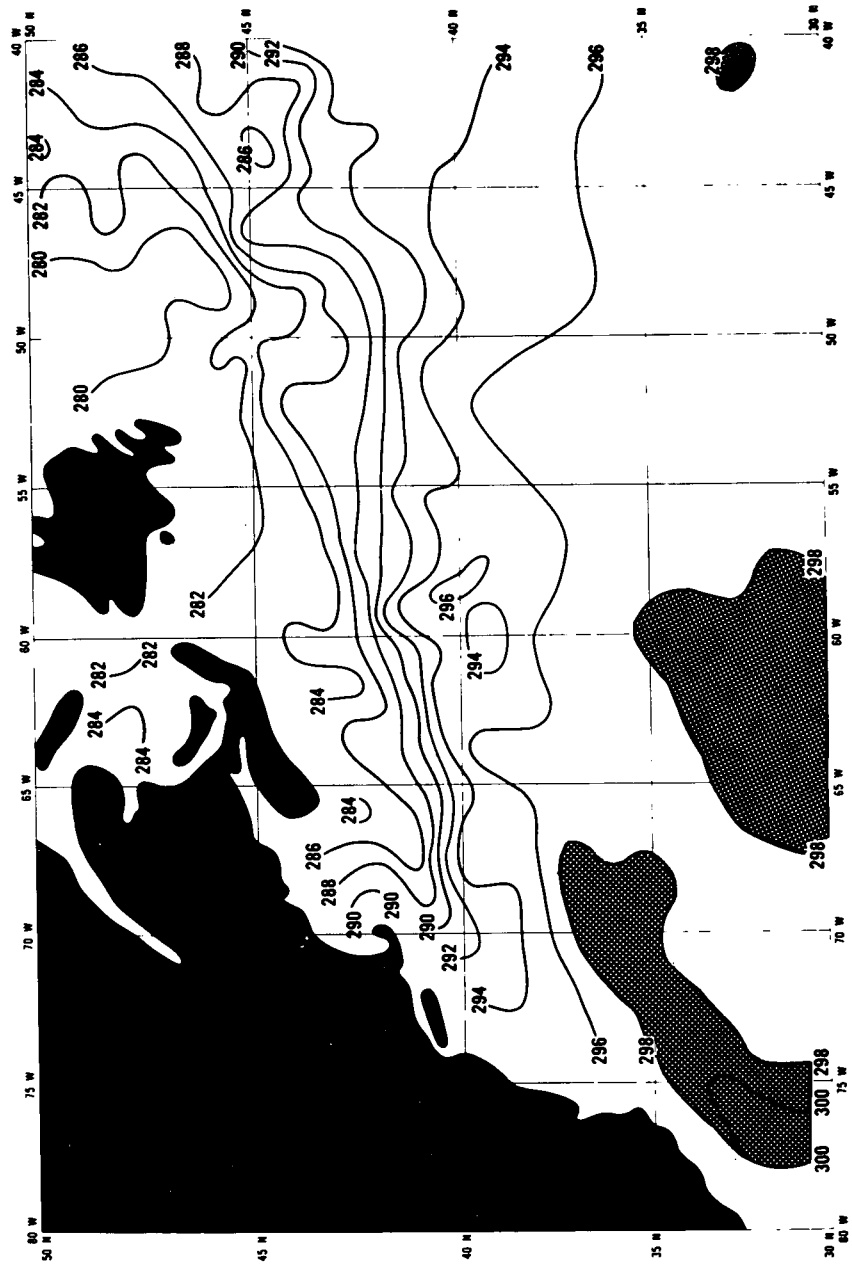

Figure 5 - Satellite generated map of sea surface temperature (mid-June to mid-July, 1966) over the western North Atlantic where the assumed cloud free 10-11 μm equivalent blackbody temperatures have been corrected for the effects of the atmosphere. Isotherms are in °K with the warmest areas (≥298°K) stippled.

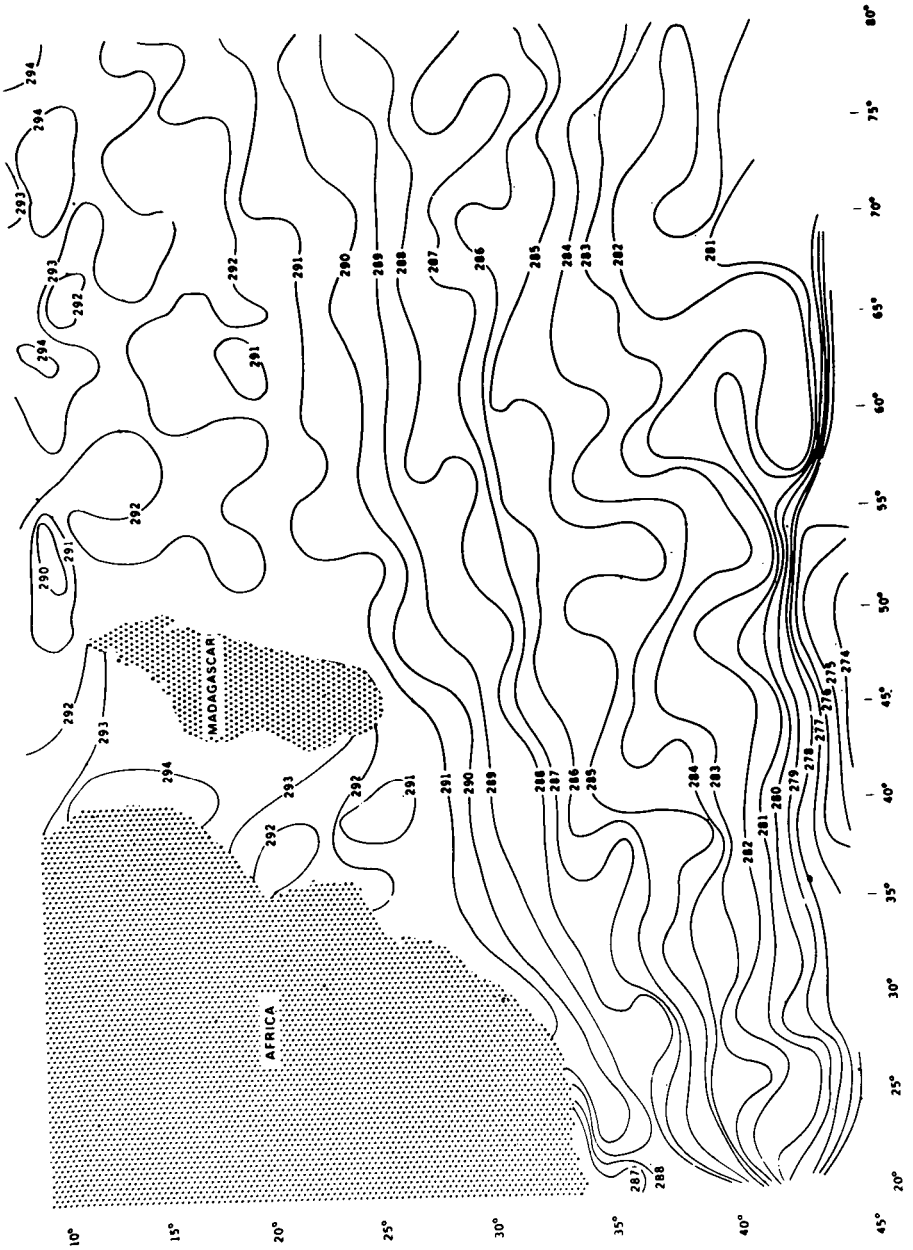

Figure 6 - June, 1966, southern Indian Ocean map of assumed cloud free 10-11 μm equivalent blackbody temperatures (°K) that are uncorrected for atmospheric effects.

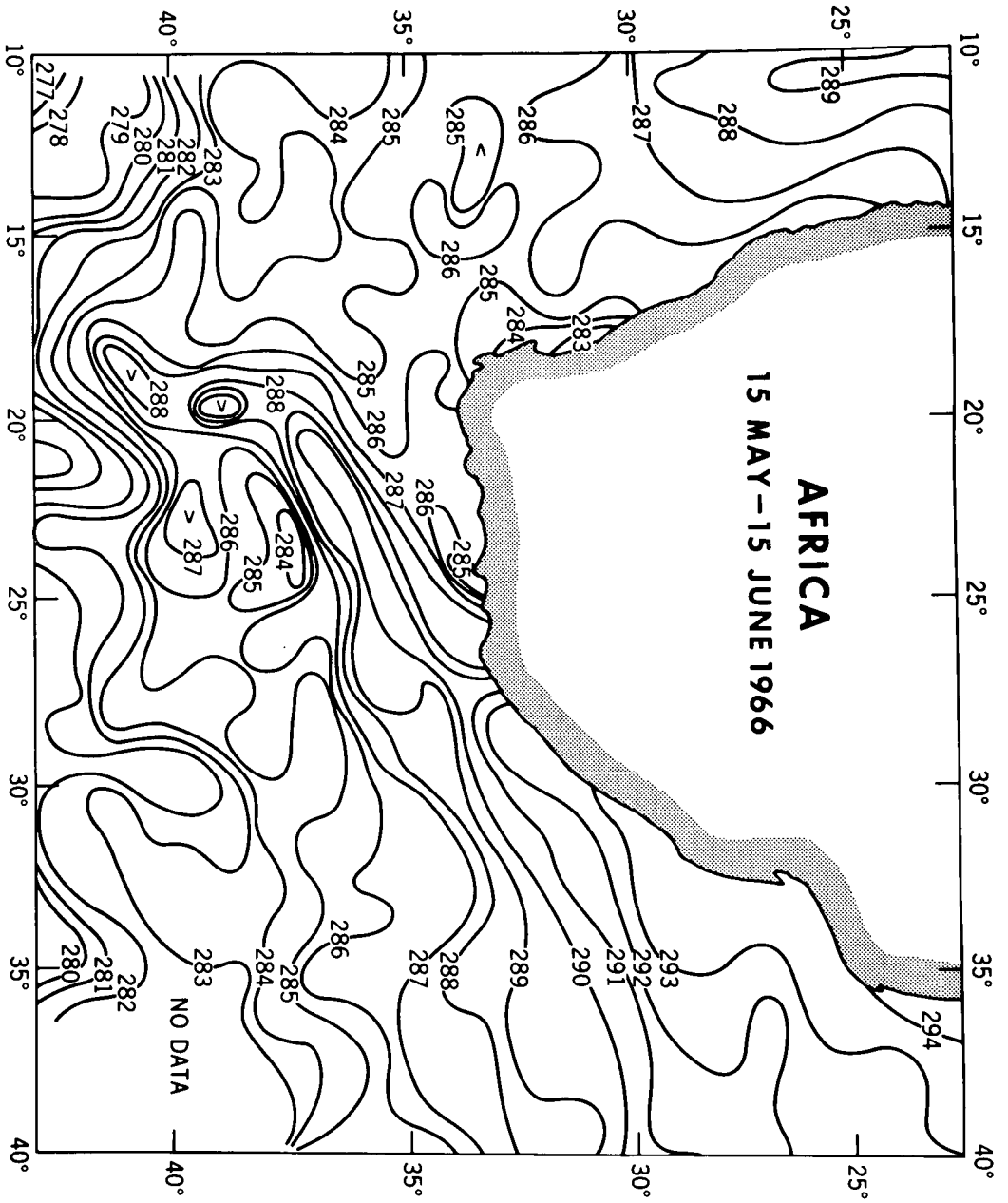

Figure 7 - Mid-May to mid-June, 1966 chart of assumed cloud free 10-11 μm equivalent blackbody temperatures (°K), uncorrected for the atmosphere, over portions of the southwestern Indian Ocean and southeastern Atlantic Ocean.